Computation of Sonar Performance Metrics Part 5

Marshall Bradley

This document illustrates how various types of uncertainty affect the forecasting of sonar performance in naval applications. The first type of uncertainty arises from the fact that we have incomplete knowledge regarding key target kinematic parameters such as range, bearing, depth, heading, speed, etc. In general key sonar performance metrics such as the sonar probability of detection P(D) are dependent upon each of these kinematic parameters. A second type of uncertainty is caused by the actual oceanographic environment in which the sonar operates. At a conceptual level, a sonar makes a mark on a gram or display when the voltage in a detector circuit exceeds a threshold. The probabilities with which these marks occur are determined by the statistics of the noise and signal that the sonar actually experiences. The statistical distribution of the signal and noise fields at the sonar receiver are strongly influenced by a nondeterministic component of ocean sound transmission. Numerous examples are presented.

Background

This document was originally written in 2010 when the author was a scholar in residence at Southeastern Louisiana University. It is presented here in a slightly updated format. In some instances the Mathematica code for computing the figures has been included. The original document contained an introduction and six sections. The author is currently the Chief Scientist at LogLinear Group, LLC.

marshall.bradley@gmail.com
September 2022

7.0 Uncertainty and Performance Prediction

7.1 Effect of error in SNR prediction on sonar performance metrics

In our previous examples we have considered the effects that the target probability density $P(r)$ has on various sonar performance metrics. We have used the target probability density $P(r)$ as a proxy for the more general case in which there is uncertainty in the range, bearing, depth and other target parameters. In this latter case we would represent the target uncertainty by the multi-dimensional probability density function $P(r, \theta, z)$. We refer to this type of uncertainty as kinematic uncertainty and it is dealt with via the process of marginalization, which is simply computing a probability by conditioning over a set of mutually exclusive, exhaustive hypotheses.

A second type of uncertainty is caused by the actual oceanographic environment in which the sonar operates. The statistical distributions of signal and noise that the sonar actually experiences are caused by a nondeterministic component of ocean sound transmission and by the random nature of background noise sources. For example, in a multipath environment, a sonar will often experience a Rayleigh fading signal with a 5.56 dB standard deviation. A sonar designer realizes this and builds a detector which maximizes sonar performance in light of the known statistical distributions of signal and noise within which the sonar will operate. From the standpoint of performance prediction, this second type of uncertainty is modeled in the mapping from sonar signal-to-noise ratio *snr* to probability of detection p_d as discussed in section 3. A sonar which is mismatched to its environment will experience diminished performance. This factor can be addressed by using the proper mapping form *snr* to p_d.

If we want to forecast sonar performance then we need to predict the signal and noise fields at the sonar receiver. Forecasting sonar performance leads to a third type of uncertainty. Due to our imperfect knowledge about the ocean environment (imperfect data bases, unknown locations of noise sources such as merchant ships, etc.), there is a degree of uncertainty associated with our performance prediction. This type of uncertainty deals with a range of possibilities, none of which can be determined from our current state of environmental knowledge.

In our treatment of kinematic variability, we have considered three basic types of performance metrics: Those that are strongly dependent on $P(r)$, those that are independent of $P(r)$ and those that are weakly dependent on $P(r)$. Representative examples of these performance metrics are the probability of detection

$$P(D) = \int_0^\infty P(D \mid r)\, P(r)\, dr,$$

the half-sweep width

$$W_{1/2} = \int_0^\infty P(D \mid r)\, dr,$$

and the Bayesian expected detection range

$$\bar{r} = \int_0^\infty r\, P(r \mid D)\, dr,$$

where $P(r \mid D)$ is the Bayesian posterior target probability density function

$$P(r \mid D) = \frac{P(D \mid r)\, P(r)}{\int_0^\infty P(D \mid r)\, P(r)\, dr}.$$

While each of these three sonar metrics depend upon the target probability density function $P(r)$ in different ways, they all are strongly dependent upon the sensor lateral range $P(D \mid r)$.

We will now consider the effect that imprecise knowledge about the ocean environment has on sonar performance prediction. This uncertainty will influence the way in which we represent sensor lateral range and as a consequence it will impact each of our three basic types of sonar performance metrics, regardless of the way in which they depend on $P(r)$. To this end, consider a sonar located at a point (x, y) in an oceanographic area of interest. We will assume that all parameters concerning the opera-

tion of the sonar, including its depth, source level, orientation, etc., are known with complete certainty. We will assume the existence of acoustic models that correctly solve the wave equation given the proper environmental inputs. We could accurately predict the probability of detection $P(D \mid x\, y\, r\, \theta\, z)$ for a target located in cylindrical coordinates (r, θ, z) measured with respect to the sonar location (x, y), if the acoustic environment was also known with complete certainty. The problem that we seek to address now is what happens when we do not completely know the oceanographic environment. In order to simplify notation, we will suppress the sonar location and address only the range component of target uncertainty. Thus in the case of complete knowledge about the acoustic environment, the sonar performance prediction model correctly predicts the lateral range curve $P(D \mid r)$.

A more realistic representation of the information obtainable from acoustic models in the presence of environmental uncertainty is to replace $P(D \mid r)$ with the probability density function $g(p_d \mid r\, U)$, where the symbol U denotes the existence of uncertainty and r is the horizontal distance from the sonar to the target. From a conceptual standpoint, you can envision $g(p_d \mid r\, U)$ as being obtained from a Monte Carlo process entailing many acoustic model runs, each performed over one of the possible acoustic environments. In the case of complete knowledge about the acoustic environment, there is only one possible environment and

$$g(p_d \mid r\, C) = \delta[p_d - P(D \mid r)],$$

where $\delta(p_d)$ is the Dirac-delta function and the symbol C represent compete knowledge of the acoustic environment. If the environmental uncertainty is small and $g(p_d \mid r\, U)$ is tightly concentrated about some measure of central tendency, then the expected probability of detection and the standard deviation of probability of detection,

$$P(D \mid r\, U) = \int_0^1 p_d\, g(p_d \mid r\, U)\, dl\, p_d,$$

$$\sigma(D \mid r\, U) = \left[\int_0^1 (p_d - \overline{p}_d)^2\, g(p_d \mid r\ U)\, dl\, p_d\right]^{1/2},$$

will provide full information about sonar performance. A generalization of the sonar probability of detection $P(D)$ in light of acoustic performance prediction model uncertainty (U) is

$$P(D \mid U) = \int_0^\infty P(D \mid r\, U)\, P(r)\, dl\, r$$

$$= \int_0^\infty \int_0^1 p_d\, g(p_d \mid r\, U)\, dl\, p_d\, P(r)\, dl\, r.$$

The Bayesian posterior target probability distribution is the target probability density given that a detection has occurred. In the absence of uncertainty U regarding the acoustic environment, this quantity is

$$P(r \mid D) = \frac{P(D \mid r)\, P(r)}{P(D)} = \frac{P(D \mid r)\, P(r)}{\int_0^\infty P(D \mid r)\, P(r)\, dl\, r}.$$

When uncertainty U regarding the acoustic environment is present, then $P(D \mid r)$ must be represented by the probability density function $g(p_d \mid r\, U)$ and the Bayesian posterior target probability distribution becomes

$$P(r \mid D\,U) = \frac{P(D \mid r\,U)\,P(r \mid U)}{P(D \mid U)}.$$

If we make use of the fact that the target probability density function $P(r)$ is independent of model uncertainty U, we obtain

$$P(r \mid D\,U) = \frac{P(D \mid r\,U)\,P(r)}{P(D \mid U)}.$$

From this it follows that Bayesian posterior target probability distribution can be written

$$P(r \mid D\,U) = \frac{\int_0^1 p_d\, g(p_d \mid r\,U)\, dl p_d\, P(r)}{\int_0^\infty \int_0^1 p_d\, g(p_d \mid r\,U)\, dl p_d\, P(r)\, dl r}.$$

When we have complete knowledge of the acoustic environment, then the U becomes C and $g(p_d \mid r\,C) = \delta[p_d - P(D \mid r)]$. In this case, the Bayesian posterior reduces to

$$P(r \mid C) = \frac{P(D \mid r)\,P(r)}{\int_0^\infty P(D \mid r)\,P(r)\, dl r}.$$

In order to illustrate the significance of uncertainty in the environment on the prediction of sensor lateral range $P(D \mid r)$, we will consider an omnidirectional passive sonar that operates in an ambient noise field with spectral noise level AN = 80 dB re 1 μPa $\Big/ \sqrt{\text{Hz}}$. The target source level is assumed to be SL = 160 dB re 1 μPa and spherical spreading transmission loss is assumed to apply between the target and the sonar. We will assume that the sonar employs a signal processor that is optimized for a Rayleigh fading signal with an integration time T = 1 sec and false alarm rate of p_{fa} = 10 ^ (–6) as described in section 5.8. If r denotes distance from the target to the sonar receiver, then the signal to noise ratio in the absence of uncertainty is

$$snr_C(r) = \frac{T\, 10^{\frac{SL}{10}}\, r_0^2}{10^{\frac{AN}{10}}\, r^2},$$

where r_0 is a reference distance. The probability of detection at a signal-to-noise ratio snr and false alarm rate p_{fa} is

$$p_d(snr, p_{\text{fa}}) = (p_{\text{fa}})^{\frac{1}{1+snr}}.$$

A plot of this function for a probability of false alarm rate p_{fa} = 10 ^ (–6) is shown in figure 7.1. At a range of 2300 yd the probability of detection is 0.5.

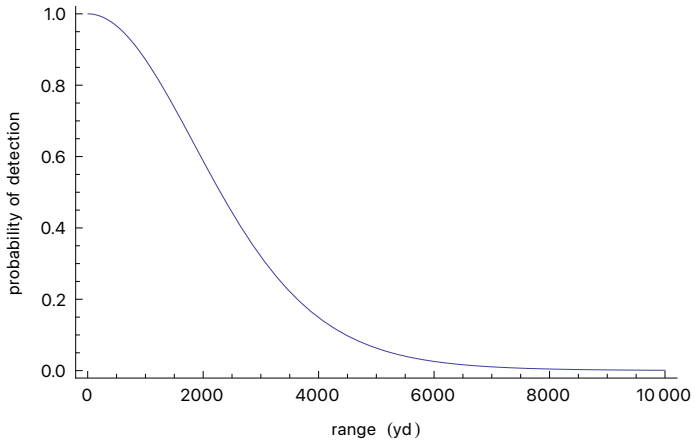

Figure 7.1. Sensor lateral range in the absence of uncertainty in the prediction of *snr*.

We will assume that the probability density function of signal-to-noise is uniformly distributed over a prescribed interval of variable width. Specifically at range r we assume that the probability density function for the sonar signal-to-noise snr is

$$f(snr \mid r) = \begin{cases} \dfrac{1}{\alpha \cdot snr_C(r) - snr_C(r)/\alpha}, & snr_C(r)/\alpha < snr < \alpha \cdot snr_C(r) \\ 0, & \text{otherwise.} \end{cases}$$

Due to the simple analytic structure of the mapping from snr to p_d, the probability density function $g(p_d \mid r\, U)$ can be found in closed form:

$$g(p_d \mid r\, U) = f[v(p_d)]\, v'(p_d) = \begin{cases} -\dfrac{1}{\alpha \cdot snr_C(r) - snr_C(r)/\alpha}\, \dfrac{\log(p_{\text{fa}})}{p_d \log(p_d)^2}, & p_{\text{d1}} < p_d < p_{\text{d2}} \\ 0, & \text{otherwise,} \end{cases}$$

where $p_{\text{d1}} = p_d(snr_C(r)/\alpha, p_{\text{fa}})$ and $p_{\text{d2}} = p_d(\alpha \cdot snr_C(r), p_{\text{fa}})$. The function $v(p_d)$ is the inverse of $p_d(snr, p_{\text{fa}})$ and is defined by the equation

$$v(p_d) = \frac{\log(p_{\text{fa}})}{\log(p_d)} - 1.$$

The amount of uncertainty in the probability density function $f(snr \mid r)$ of signal-to-noise ratio at range r is controlled by the parameter α. The interval $(snr_C(r)/\alpha, \alpha \cdot snr_C(r))$ when converted to a decibel scale is $(SNR_C(r) - 10\log\alpha, SNR_C(r) + 10\log\alpha)$. We will use values of the parameter α equal to 1.122, $\sqrt{2}$, 2 and 4, corresponding to decibel (dB) widths of ±0.5, ±1.5, ±3 and ±6 dB in the distribution of signal-to-noise ratio snr.

Plots of the probability density function $g(p_d \mid r\, U)$ for four levels of uncertainty are shown in figure 7.2 at a range of 2300 yd. If there is no environmental uncertainty, then at a range of 2300 yd the probability of detection is 0.5. Note how each of the four probability distributions is centered on $p_d = 0.5$. As the uncertainty decreases the probability density functions become more peaked with the density concentrated within a narrower range.

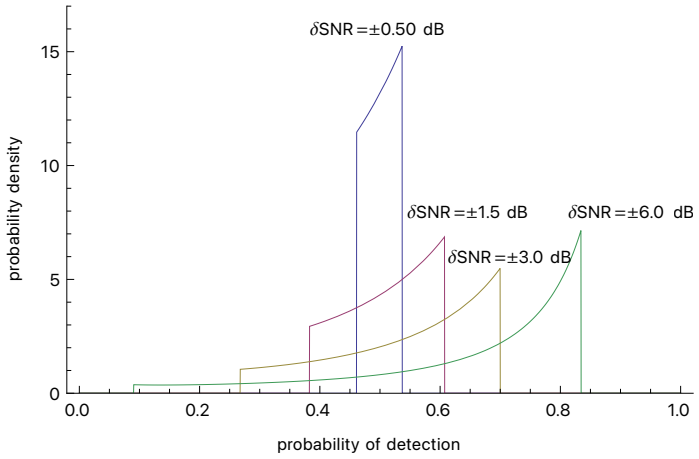

Figure 7.2. Distribution of probability of detection at r = 2300 yd. In the absence of uncertainty, the probability of detection at this range is 0.50. As uncertainty decreases the probability density function tends to a Dirac-delta function.

A quantitative measure of the uncertainty in a probability distribution is the entropy S. In this particular case the appropriate definition for entropy is

$$S = -\int_0^1 g(p_d \mid r\, U) \log[g(p_d \mid r\, U)]\, d p_d.$$

A computation of this function at a range of 2300 yd is shown in figure 7.3. As expected, entropy increases with increasing uncertainty. Figure 7.4 shows computations of entropy at ranges from 500 to 6000 yds. Entropy is maximal at ranges from 2300 to 3500 yd, depending upon uncertainty level. This range band corresponds to the signal-to-noise range where probability of detection is most rapidly decreasing as shown in figure 7.1. At very short ranges and at longer ranges entropy decreases since probability of detection density becomes concentrated near 0 or 1 respectively in these two cases.

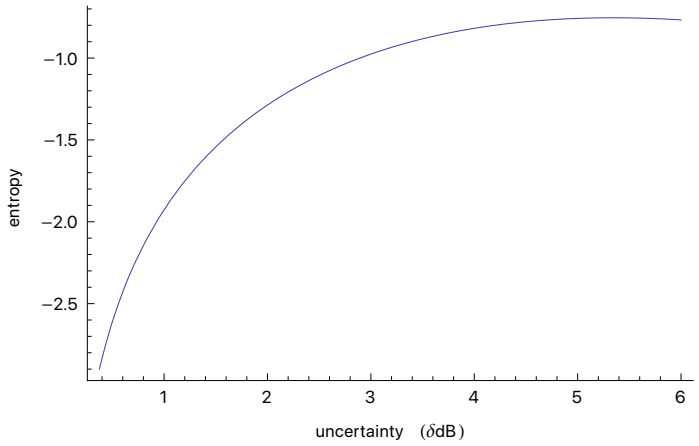

Figure7.3. Entropy at r = 2300 yd with increasing levels of uncertainty. The probability of detection at this range is 0.5.

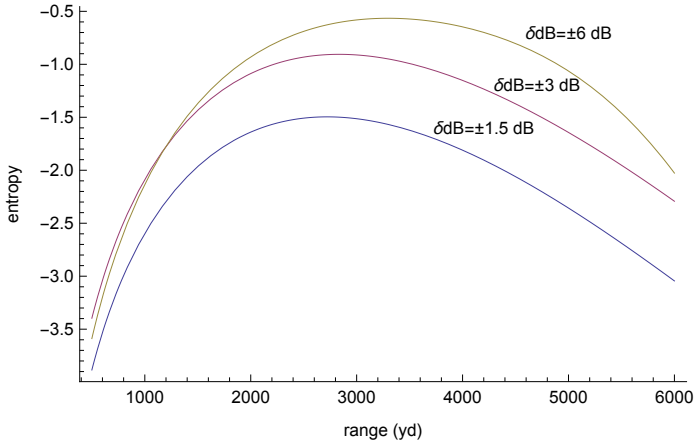

Figure 7.4. Entropy as a function of range for three levels of uncertainty.

We now turn our attention to the effects that uncertainty has on sensor lateral range. Figure 7.5 shows plots of the expected probability of detection as a function of range

$$P(D \mid r\,U) = \int_0^1 p_d\, g(p_d \mid r\,U)\, dl p_d,$$

which is the generalization of lateral range in the presence of uncertainty in *snr*. The curve labeled with δdB = 0 is the lateral range curve $P(D \mid r)$ in the absence of uncertainty. Note how probability of detection becomes strongly positively biased for the larger uncertainty value δdB = ±6 dB. An explanation of this phenomena is provided in figure 7.6. This latter figure shows the distribution of probability of detection at two levels of uncertainty at a range of 6000 yd. The probability density function at the larger uncertainty value δdB = ±6 has a long tail to the right containing a significant amount of probability density. This tail will provide a significant positive bias to any sonar metrics estimated from the probability density function $g(p_d \mid r\,U)$.

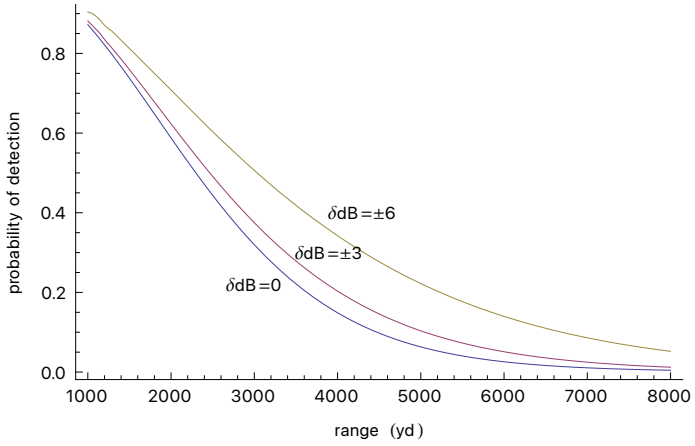

Figure 7.5. Effect of uncertainty on sonar lateral range.

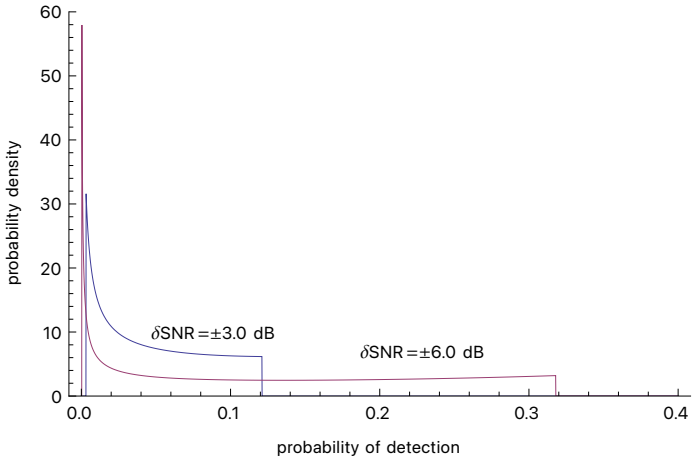

Figure 7.6. Distribution of probability of detection at r = 6000 yd.

Figure 7.7 shows the effects of uncertainty in *snr* on the Bayesian posterior probability density function

$$P(r \mid D\,U) = \frac{\int_0^1 p_d\, g(p_d \mid r\,U)\, dl\, p_d\, P(r)}{\int_0^\infty \int_0^1 p_d\, g(p_d \mid r\,U)\, dl\, p_d\, P(r)\, dl\, r}.$$

The bias that we saw in the lateral range curves towards higher probabilities of detection with an increase in uncertainty now materializes as a bias towards longer detection ranges in the Bayesian posterior probability distributions.

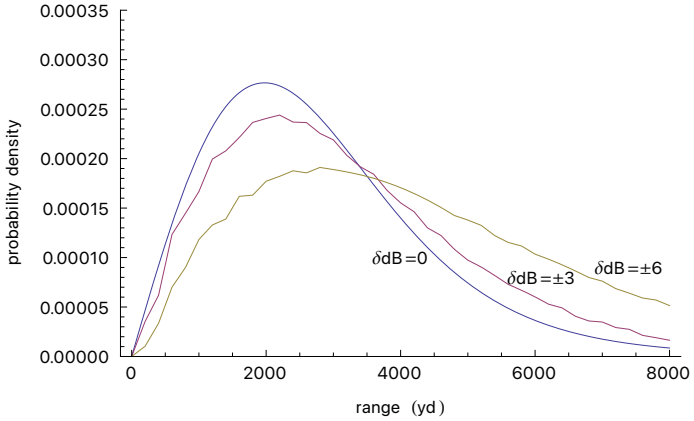

Figure 7.7. Effect of uncertainty on Bayesian posterior.

Table 7.1 shows the effects of uncertainty in the prediction of *snr* on the sonar performance metrics probability of detection $P(D)$, half-sweep width $W_{1/2}$ and the Bayesian expected detection range $\bar{r}$. This latter parameter is the expected detection range given that a sonar detection has occurred. For the larger value of uncertainty δdB = ±6 there is a significant effect on all sonar performance metrics.

Metric	*δdB=0*	*δdB = ± 1.5*	*δdB = ±3*	*δdB=±6*
$P(D)$	0.133	0.140	0.163	0.252
$W_{1/2}$	2530 yd	2601 yd	2779 yd	3449 yd
$\bar{r}$	2746 yd	2838 yd	3089 yd	3770 yd

Table 7.1. Effect on uncertainty in the prediction of *snr* on the sonar performance probability of detec-

tion $P(D)$, half-sweep width $W_{1/2}$ and the Bayesian expected detection range $\bar{r}$ which is the expected detection range given that a detection has occurred.

7.2 Distribution of probability of detection with normal distributed uncertainty

Suppose that the sonar equation has been solved for the decibel signal to noise ratio *SNR* present at the detector input of a sonar. Further assume that there is some uncertainty associated with this computation of *SNR*. If we let X denote the *SNR*, then a plausible initial assumption is that the random variable X is normally distributed with probability density function

$$h(x, \mu, \sigma) = \frac{1}{\sqrt{2\,\pi}\;\sigma}\,\exp\Big[-\frac{(x-\mu)^2}{2\,\sigma^2}\Big],$$

where μ is the mean decibel *SNR* level predicted by the modelling process and σ is the measure of the decibel uncertainty associated with the prediction. For instance, in a situation where acoustic performance prediction models predict favorable sonar performance with a great deal of certainty, we might have $\mu = 17$ dB and $\sigma = 1$ dB. If the random variable X is not normally distributed then the following arguments can be readily modified to accommodate this piece of a priori information, provided that the probability density function of X is known. If we let the random variable Y denote the signal to noise ratio measured on an intensity scale, then the relationship between the random variables X and Y is

$$Y = 10^{\frac{X}{10}},\; X = 10\log_{10}(Y).$$

The random variable Y is said to have a lognormal distribution and its probability density function is

$$f(y, \mu, \sigma) = \frac{1}{\sqrt{2\,\pi}\;\sigma}\,\frac{10}{\log(10)}\,\frac{1}{y}\,\exp\Big[-\frac{(10\log_{10}(y)-\mu)^2}{2\,\sigma^2}\Big].$$

The probability density functions $h(x, \mu, \sigma)$ and $f(y, \mu, \sigma)$ convey the same information about the uncertainty in *SNR*, only the scales are different. *SNR* when measured on an intensity scale is defined on the interval $0 \le y < \infty$. If we measure *SNR* on a decibel scale then it is defined on the interval $-\infty < x < \infty$. The condition of absolutely no signal corresponds to $y = 0$ or $x = -\infty$. Infinite signal corresponds to infinity on both scales.

If we assume that the sonar is optimized for a signal with random phase and Rayleigh amplitude, then the appropriate mapping from *SNR* to probability of detection p_d is (Whalen, 1971)

$$p_d(y, p_{\text{fa}}) = (p_{\text{fa}})^{\frac{1}{1+y}},$$

where p_{fa} is the sonar false alarm rate and y is the *SNR* measured on an intensity scale.

At this point it is important to emphasize that we are addressing two fundamentally different types of uncertainty. The first of these is associated with the random nature of the signal and noise fields in which the sonar actually operates. Whalen's detection model assumes that the signal phase is randomly distributed over the interval $(0, 2\,\pi)$ and the signal amplitude is Rayleigh distributed with probability density function

$$w(A) = \frac{A}{A_0^2} \exp\left[-\frac{A}{2 A_0^2}\right],\ A \geq 0.$$

Additionally it is assumed that the noise in the sonar detection circuit is white with constant spectral density N_0. The signal to noise ratio y is

$$y = \frac{A_0^2 T}{N_0},$$

where T is the integration time of the sonar detector. The optimum receiver in this case is a matched filter followed by an envelope detector. Knowledge of the signal phase or amplitude is not required to achieve optimum performance. Only the properties of the noise must be known to set a detection threshold at an appropriate false alarm rate.

The second type of uncertainty addresses the fact that we cannot predict the signal to noise ratio y with 100% certainty. We represent this second type of uncertainty via the probability density function $h(x, \mu, \sigma)$ or equivalently via $f(y, \mu, \sigma)$. The second type of uncertainty arises from our imprecise knowledge of the ocean environment. Kinematic uncertainty regarding the position, depth, range, heading, etc. of the target can be incorporated into $h(x, \mu, \sigma)$ as well. If we convert the intensity *SNR* to a decibel scale we have

$$X = 10 \log(A_0^2) - 10 \log(N_0) + 10 \log(T),$$

or more generally

$$X = SL - TL - AN + PG.$$

Thus in a practical situation, the random variable X is the sum of several independent (hopefully) random variables. Even if these random variables are uniformly distributed, the processes of finding the probability density function $h(x, \mu, \sigma)$ via multiple convolutions will result in a distribution that is approximately bell shaped. An example of this type of computation was presented in section 4.4.

We now again turn our attention to the probability distribution of the probability of detection. Whalen's function $p_d(y, p_{\text{fa}})$ is a monotonic increasing map from intensity *SNR* to probability of detection. It has inverse function

$$v(p_d, p_{\text{fa}}) = \frac{\log(p_{\text{fa}})}{\log(p_d)} - 1,$$

with derivative

$$v'(p_d, p_{\text{fa}}) = -\frac{\log(p_{\text{fa}})}{p_d \log^2(p_d)}.$$

Because of the simple properties of the inverse function $v(p_d, p_{\text{fa}})$, the probability density function $g(p_d, p_{\text{fa}}, \mu, \sigma)$ of probability of detection p_d can be found in closed form. The result is

$$g(p_d, p_{\text{fa}}, \mu, \sigma) = f[v(p_d, p_{\text{fa}}) \mu, \sigma]\, v'(p_d, p_{\text{fa}})$$

or more completely

$$g(p_d, p_{\text{fa}}, \mu, \sigma) = -\left(5\, e^{-\frac{\left(-\mu + \frac{10\,\text{Log}\left[-1 + \frac{\text{Log}[p_{\text{fa}}]}{\text{Log}[p_d]}\right]}{\text{Log}[10]}\right)^2}{2\,\sigma^2}} \sqrt{\frac{2}{\pi}}\, \text{Log}[p_{\text{fa}}]\right) \Big/ \left(\sigma\, \text{Log}[10]\, \text{Log}[p_d]^2 \left(-1 + \frac{\text{Log}[p_{\text{fa}}]}{\text{Log}[p_d]}\right) p_d\right),\ p_{\text{fa}} \le p_d \le 1.$$

Plots of the probability density function $g(p_d, p_{\text{fa}}, \mu, \sigma)$ of probability of detection p_d are shown in figure 7.7 for $\mu = 12.78$ dB and a false alarm rate of $p_{\text{fa}} = 10\,\text{^}\,(-6)$ and a range of values of σ. The value $\mu = 12.78$ dB corresponds to a 50% probability of detection ($p_d = 0.50$). Referring to figure 7.7, when $\sigma = 0.5$, 1 and 2 dB, $g(p_d, p_{\text{fa}}, \mu, \sigma)$ is peaked at values of probability of detection near $p_d = 0.50$. For larger values of σ, the probability density function $g(p_d, p_{\text{fa}}, \mu, \sigma)$ is quite spread out across the interval (0,1). In order to better observe the spread in probability of detection and its sensitivity to σ, figure 7.8 shows a computation of the probability density function $g(p_d, p_{\text{fa}}, \mu, \sigma)$ with the horizontal axis expressed on a logarithmic scale. Somewhere between $\sigma = 2$ dB and $\sigma = 8$ dB, the probability density function $g(p_d, p_{\text{fa}}, \mu, \sigma)$ undergoes a significant change in character.

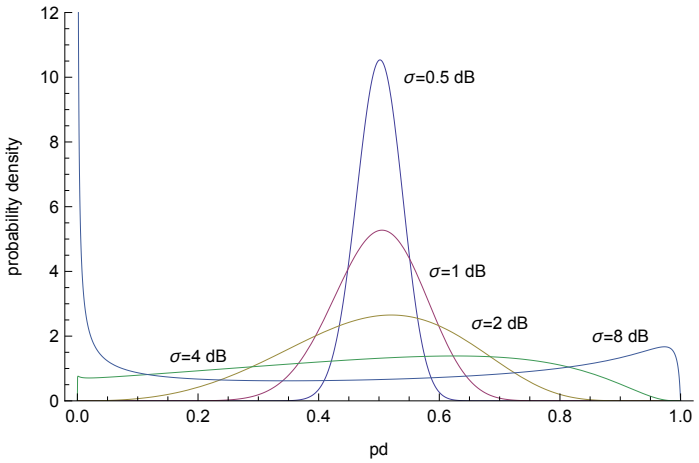

Figure 7.7. Computation of the probability density function $g(p_d, p_{\text{fa}}, \mu, \sigma)$ for $\mu = 12.78$ dB, $p_{\text{fa}} = 10\,\text{^}\,(-6)$ and a range of values of σ. The value $\mu = 12.78$ dB corresponds to a 50% probability of detection ($p_d = 0.50$) in the absence of predictive uncertainty ($\sigma = 0$). The distribution in uncertainty in *SNR* has been assumed to be normal.

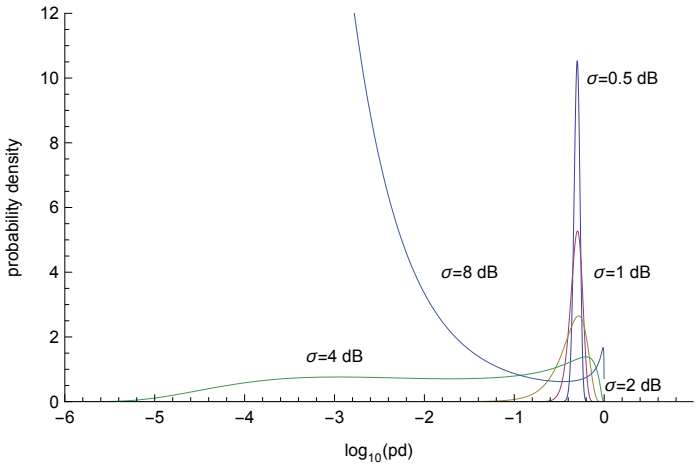

Figure 7.8. Computation of the probability density function $g(p_d, p_{fa}, \mu, \sigma)$ for $\mu = 12.78$ dB, $p_{fa} = 10\text{^}(-6)$ and a range of values of σ. The value $\mu = 12.78$ dB corresponds to a 50% probability of detection ($p_d = 0.50$) in the absence of predictive uncertainty ($\sigma = 0$). The horizontal axis is on a logarithmic scale.

In order to gain further insight into the character of the probability density function $g(p_d, p_{fa}, \mu, \sigma)$ and its sensitivity to the uncertainty parameter σ, we need a mathematical measure of the amount of disorder in a probability distribution. The entropy of the probability distribution is the appropriate measure of disorder in this case. Mathematically, the entropy of any continuous probability distribution is

$$S = -\int p(x) \log[p(x)]\, dx,$$

where $p(x)$ is the probability density function of the distribution and the integral is computed over the range of support for $p(x)$. Relatively speaking, very peaked probability distributions have significantly less entropy than more evenly shaped (uniform) probability distributions. For a normal probability distribution with mean μ and standard deviation σ, the entropy depends only on the standard deviation and is given by

$$S_{normal}(\sigma) = -\int_{-\infty}^{\infty} \frac{1}{\sqrt{2\pi}\,\sigma} e^{\frac{-(x-\mu)}{2\sigma^2}} \log\left[\frac{1}{\sqrt{2\pi}\,\sigma} e^{\frac{-(x-\mu)}{2\sigma^2}}\right] dx = 1.41893 + \log(\sigma),$$

where 1.41893 is the entropy of a normal distribution with standard deviation equal to one. Thus for a normal distribution, as the standard deviation σ increases so does the entropy.

Figure 7.9 shows the relationship between the entropy of *SNR* and the entropy of the probability of detection. The figure is a parametric plot of the form

$$\left\{1.41893 + \log(\sigma), -\int_0^1 g(p_d, p_{fa}, \mu, \sigma) \log[g(p_d, p_{fa}, \mu, \sigma)]\, dp_d\right\}.$$

The mean *SNR* level has been chosen to be $\mu = 12.78$ dB corresponding to a 50% probability of detection at a false alarm rate of $p_{fa} = 10\text{^}(-6)$. The standard deviation σ of the *SNR* has been varied from 1 to 8 dB. Initially, the entropy of SNR and the entropy of p_d have a positive linear relationship. However

when the *SNR* distribution becomes sufficiently disordered, the entropy of p_d begins to decrease as the underlying distribution of p_d becomes more peaked at the tails as shown in figure 1. The maximum in the entropy of p_d occurs when the entropy of the *SNR* is about 3. This corresponds to $\sigma = 4.9$ dB. Thus if the underlying *SNR* distribution has a standard deviation in excess of about 4.9 dB, then the resulting distribution of p_d has so much probability in the tails near $p_d = 0$ and $p_d = 1$ that the entropy of the probability distribution begins to decrease rather than increase with increasing entropy in *SNR*. Maximum entropy in the distribution of probability of detection is not desirable.

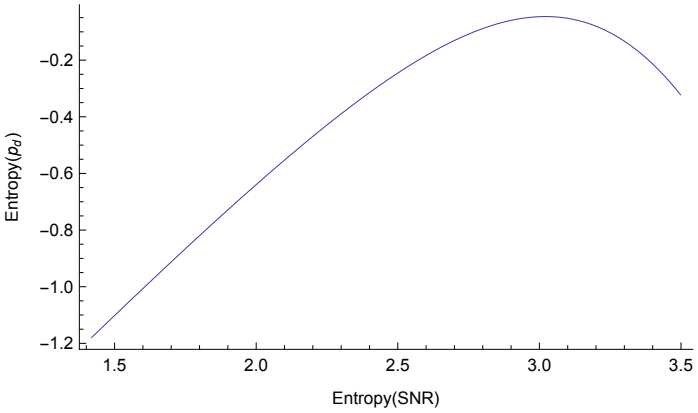

Figure 7.9. Parametric plot of entropy of *SNR* versus entropy of probability of detection for $\mu = 12.78$ dB and a false alarm rate $p_{fa} = 10\,\text{^}\,(-6)$. The *SNR* value $\mu = 12.78$ dB corresponds to a 50% probability of detection.

We now turn our attention to the effect of uncertainty in *SNR* on the mean of the distribution of probability of detection. The expected value of probability of detection is defined to be

$$\overline{p}_d = E[p_d] = \int_{p_{fa}}^{1} p_d \, g(p_d, p_{fa}, \mu, \sigma) \, dp_d.$$

This integral is mathematically equivalent to

$$E[p_d] = \int_{0}^{\infty} (p_{fa})^{\frac{1}{1+y}} f(y, \mu, \sigma) \, dy,$$

which in turn is equivalent to the integral

$$E[p_d] = \int_{-\infty}^{\infty} (p_{fa})^{\frac{1}{1+10^{\frac{x}{10}}}} h(x, \mu, \sigma) \, dx,$$

where this last integral is computed over a range of decibel levels.

Computations of the mean probability of detection $E[p_d]$ are shown in figure 7.10 for mean *SNR* levels μ equal to 9.53, 12.78 and 16.73 dB. In the absence of uncertainty ($\sigma = 0$) these mean *SNR* levels correspond to probabilities of detection 0.25, 0.50 and 0.75. As uncertainty increases, the mean probability of detection tends to 50%, regardless of the mean *SNR* level.

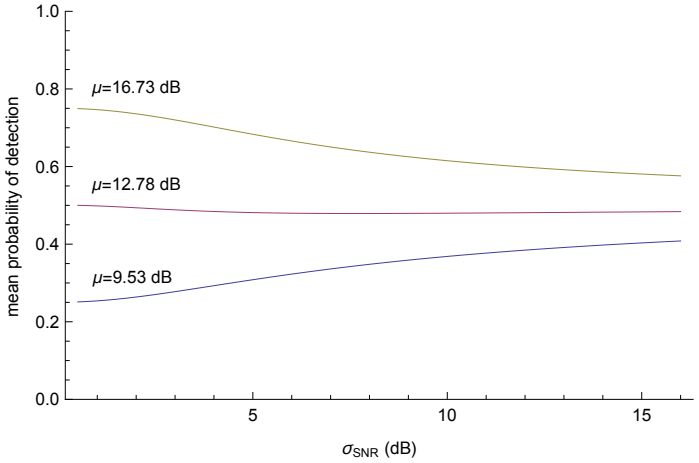

Figure 7.10. Computation of mean probability of detection for mean signal to noise ratios $\mu = 9.53,\ 12.78$ and 16.73 dB with $p_{fa} = 10\,\text{^}\,(-6)$ as a function of σ, the standard deviation of *SNR*. These values of μ correspond to probability of detection p_d equal to 0.25, 0.50 and 0.75 in the absence of predictive uncertainty ($\sigma = 0$) in the *SNR*.

Figure 7.11 shows 90% confidence levels for the probability of detection p_d as a function of the standard deviation σ of the SNR level for mean SNR levels μ equal to 9.53, 12.78 and 16.73 dB. In the absence of uncertainty ($\sigma = 0$) these mean SNR levels correspond to probabilities of detection 0.25, 0.50 and 0.75. There are three families of curves in the figure. The lower and upper curves in each family are the lower and upper bounds of the probability of detection confidence interval. There is a 90% chance that the true value of probability of detection will fall between these limits. These curves have been found by exploiting the fact that 90% of the area in a normal distribution lies within the symmetric interval $(\mu - 1.645\,\sigma,\ \mu + 1.645\,\sigma)$. The upper and lower bounds of probability of detection are

$$p_{d,\text{lower}}(\mu, \sigma, p_{fa}) = (p_{fa})^{\frac{1}{1+10^{\frac{\mu - z_c\,\sigma}{10}}}},\quad p_{d,\text{upper}}(\mu, \sigma, p_{fa}) = (p_{fa})^{\frac{1}{1+10^{\frac{\mu + z_c\,\sigma}{10}}}},$$

where $z_c = 1.645$. Confidence intervals for probability of detection at other levels of statistical significance can be found by changing the parameter z_c. For instance, a 95% probability of detection confidence interval requires $z_c = 1.96$. Figure 7.11 clearly demonstrates that accurate estimates of probability of detection can only be made when the uncertainty in the *SNR* estimate is relatively small.

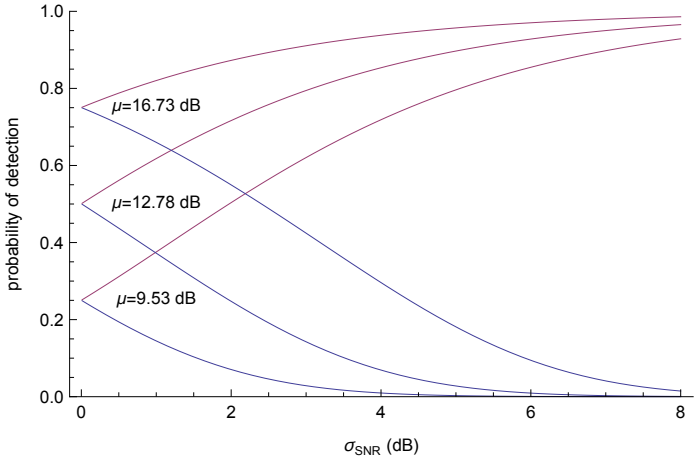

Figure 7.11. Ninety percent confidence intervals for the probability of detection when the mean signal to noise ratio is $\mu = 9.53,\ 12.78$ and 16.73 dB with $p_{fa} = 10\,\text{^}\,(-6)$. These values of μ correspond to probabilities of detection p_d equal to 0.25, 0.50 and 0.75 in the absence of predictive uncertainty ($\sigma = 0$) in the *SNR*.

For instance when $\mu = 9.53$ dB and $\sigma = 4.0$ dB, the nominal value of probability of detection is $p_d = 0.25$. However, from a statistical standpoint you can only be 90% confident that the true probability of detection lies in the interval (0.01, 0.72). As σ increases or as the requirement for higher levels of confidence increases, the situation becomes worse. When $\sigma =$ 8 dB, the 90% confidence interval is (0.00, 0.93). Predictions with this wide a range in probability uncertainty essentially carry no information.

7.3 Modeling uncertainty with the gamma distribution

In many circumstances the sonar equation when expressed on an intensity scale can be written as the ratio $U = X/Y$ where X is the signal and Y is the noise (or more generally the mask). Without any physical justification we will assume that X and Y are random variables with probability density functions $f(x)$ and $g(y)$ and furthermore assume that X and Y are distributed in accordance with a gamma distribution. Specifically we assume that the probability density functions of the signal and noise are

$$f_s(x, \alpha, \beta) = \frac{x^{\alpha-1}}{\beta^{\alpha}\,\Gamma[\alpha]}\,\exp(-x/\beta),\ 0 \le x < \infty,$$

$$f_n(y, a, b) = \frac{y^{a-1}}{b^{a}\,\Gamma[a]}\,\exp(-y/\beta),\ 0 \le y < \infty,$$

where $\Gamma(\alpha)$ denotes the gamma function evaluated at α. If n is a positive integer, $\Gamma(n) = (n-1)!$. The assumption of the gamma distribution implies that the mean signal and noise are $\alpha\beta$ and ab and that the standard deviation of the signal and noise are $\sqrt{\alpha}\ \beta$ and $\sqrt{a}\ b$.

If X and Y are positive random variables with joint density $f_{XY}(x, y)$, then the probability density function $h(u)$ of the random variable $U = X/Y$ is

$$h(u) = \int_0^\infty f_{XY}(uv, v)\, v\, dv,$$

provided that X and Y are continuous, (Milton and Arnold, 2003). If we further assume that the signal and noise X and Y are independent then we can write

$$h(u) = \int_0^\infty f_s(uy, \alpha, \beta)\, f_n(y, a, b)\, y\, dy,$$

which is the equivalent of convolution for products. Because of the properties of the gamma probability density function, this integral can be evaluated in closed form to yield the analytic representation

$$h(u, \alpha, \beta, a, b) = \frac{\beta^a\, b^\alpha\, u^{\alpha-1}\, \Gamma(a+\alpha)\, (b\,u+\beta)^{-a-\alpha}}{\Gamma(a)\, \Gamma(\alpha)}$$

of the probability density of the signal to noise ratio $U = X/Y$. The mean of the signal to noise ratio is

$$\overline{u} = \frac{\alpha\, \beta}{(a-1)\, b},\ a > 1,\ b > 0$$

A plot of the probability density function $h(u, \alpha, \beta, a, b)$ of the signal to noise intensity ratio with α=5, β=10, a = 5 and b = 1 is shown in figure 7.12.

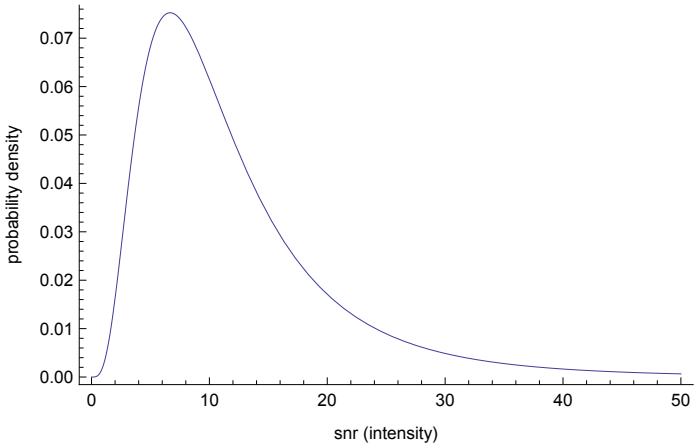

Figure 7.12 Probability density function $h(u, \alpha, \beta, a, b)$ of the signal to noise intensity ratio with α=5, β=10, a = 5 and b = 1.

If we assume a sonar that is optimized for a signal with random phase and Rayleigh amplitude, then the appropriate mapping from signal to noise ratio $U = X/Y$ to probability of detection p_d is

$$p_d(u, p_{\text{fa}}) = (p_{\text{fa}})^{\frac{1}{1+u}},$$

where p_{fa} is the sonar false alarm rate and u is the signal to noise ratio measured on an intensity scale. In this case the probability density function of probability of detection can be found in closed form. Examples of this process have been given in previous sections. Figure 7.13 shows plots of the probability density function of probability of detection at signal states β=5, 10 and 50 and with α=5, a = 5 and b = 1 (all three cases). The three signal states correspond to mean signal to noise ratios 6.25, 12.5 and 62.5. These probability density functions exhibit a substantially different character in comparison to the probability distributions discussed in the previous section where it was assumed that the signal to noise ratio in decibel space was normally distributed. The difference in character can be attributed to

different characteristics of the tails in the uncertainty distributions.

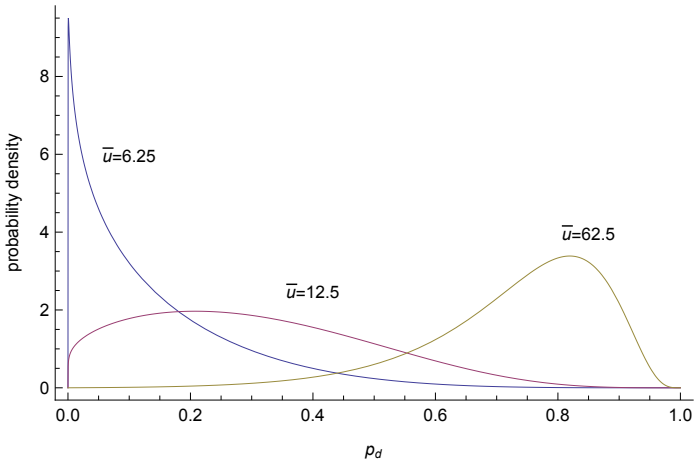

Figure 7.13 Probability density function of the probability of detection at signal states β=5, 10 and 50 and with α=5, a = 5 and b = 1 (all three cases). The three signal states correspond to mean signal to noise ratios 6.25, 12.5 and 62.5.

7.4 A Practical Approach to Representing Uncertainty in Performance Prediction Computations

In any situation in which uncertainty exists regarding the constituent terms in the sonar equation, probability of detection is a random variable. If the probability density function $g(p_d)$ of probability of detection is available, then the mean and variance of probability of detection are

$$\overline{p}_d = \int_0^1 p_d\, g(p_d)\, dp_d, \quad \sigma_{p_d}^2 = \int_0^1 (p_d - \overline{p}_d)^2\, g(p_d)\, dp_d.$$

The integral defining the variance can be expanded to yield a result that is often more computationally convenient:

$$\sigma_{p_d}^2 = \int_0^1 p_d^2\, g(p_d)\, dp_d - \overline{p}_d^2.$$

If we write the intensity signal to noise ratio in the sonar equation in the form $U = X/Y$ where X is a random variable representing signal and Y is a random variable representing mask, then the mean and variance of probability of detection can also be computed via

$$\overline{p}_d = E[P(D \mid x\, y)] = \int_0^\infty \int_0^\infty P(D \mid u = x/y)\, w(x, y)\, dx\, dy,$$

$$\sigma_{p_d}^2 = E\left[P(D \mid x\, y)^2\right] - (E[P(D \mid x\, y)])^2 = \int_0^\infty \int_0^\infty P(D \mid u = x/y)^2\, w(x, y)\, dx\, dy - \overline{p}_d^2,$$

where $w(x, y)$ is the joint probability distribution of the random variables X and Y. If these two random variables are independent, then the joint probability distribution $w(x, y)$ can be written as the product of a function of x times a function of y. That is to say $w(x, y) = s(x)\, m(y)$, where $s(x)$ and $m(y)$ are the probability densities of signal and mask.

This is an important point. At any stage of the performance prediction process where we marginalize over uncertainty to calculate a measure of central tendency such as the mean probability of detection

$\overline{p}_d$, we can also calculate the variance (or standard deviation) of this quantity as well. The amount of additional computation required is small but the potential payoff can be quite large.

Computing the standard deviation of probability of detection allows us to compute confidence intervals for probability of detection even when the probability density function $g(p_d)$ is not known. Chebyshev's theorem tell us that

$$P(\mid p_d - \overline{p}_d \mid \geq k\,\sigma_{p_d}) \leq \frac{1}{k^2},$$

for any positive number k provided that the standard deviation σ_{p_d} is finite, regardless of the details of the probability density function $g(p_d)$. Thus the interval $(\overline{p}_d - 2\,\sigma_{p_d}, \overline{p}_d + 2\,\sigma_{p_d})$ is at least a 75% confidence interval for the true value of probability of detection. If p_d were normally distributed (and there is absolutely no reason to believe that it is), the interval $(\overline{p}_d - 2\,\sigma_{p_d}, \overline{p}_d + 2\,\sigma_{p_d})$ would actually be a 95.44% confidence interval.

Often in the sonar performance prediction process, spatial maps of the mean (expected) probability of detection are presented in order to convey to the reader some sense as to how the sonar can be expected to perform as a function of location. It might be beneficial to present a map of σ_{p_d}as well so that the reader has some sense of the reliability of the numbers. Alternatively, one could define a positive spatial measure of effectiveness

$$MOE(\overline{p}_d, \sigma_{p_d}) = \frac{\overline{p}_d}{1 + \alpha\,\sigma_{p_d}},$$

where α is a positive constant (perhaps 2). This measure of effectiveness penalizes large values of uncertainty (large σ_{p_d}) and rewards certainty (small σ_{p_d}).

In order to fully illustrate the effect of the various types of uncertainty on the prediction of sensor lateral range $P(D \mid r)$ and related quantities, we will consider a passive sonar example that incorporates each of the three types of uncertainty that we have discussed. The first type of uncertainty is kinematic uncertainty. The range, bearing and depth of the target are assumed to be unknown. We will specifically assume that the target is uniformly distributed in range and bearing out to a distance $r_{\max}$. This leads to a target prior range distribution of the form

$$P(r) = \frac{r}{\frac{1}{2}\,r_{\max}^2}.$$

We will incorporate the effect of the target depth uncertainty in our representation of transmission loss.

The second type of uncertainty involves the actual distributions of signal and noise at the sonar receiver at the time of detection. We will address this second type of uncertainty by assuming that the passive sonar employs a signal processor that is optimized for detecting a Rayleigh fading signal in white noise as described in section 5.8. If r denotes distance from the target to the sonar receiver, then the signal to noise intensity ratio at the sonar is

$$snr(r) = \frac{T\, 10^{\frac{SL - TL(r)}{10}}}{10^{\frac{AN}{10}}},$$

where TL(r) is the decibel transmission loss at range r, AN is the ambient noise level and T is the sensor integration time. The probability of detection at the signal-to-noise ratio snr and false alarm rate p_{fa} is

$$p_d(snr, p_{\text{fa}}) = (p_{\text{fa}})^{\frac{1}{1+snr}}.$$

In our example we assume that the target source level is SL = 160 dB re 1 μPa, that the sonar operates in an ambient noise field with spectral noise level AN = 80 dB re 1 μPa $/\sqrt{\text{Hz}}$, that the sensor integration time is T = 1 sec, and that the false alarm rate is p_{fa} = 10^(−6).

The third type of uncertainty addresses the fact that we cannot predict the mean transmission loss and ambient noise with 100% certainty. We will assume that the transmission loss between the source and receiver is described by a Gumbel-type extreme value distribution as discussed in section 5.3. The probability density of transmission loss is

$$f_{TL}(TL, \alpha, \beta) = \frac{e^{-e^{\frac{-(TL-\alpha)}{\beta}} + \frac{-(TL-\alpha)}{\beta}}}{\beta}$$

where $\alpha(r)$ is the modal transmission loss at range r in decibel units,

$$\alpha(r) = \begin{cases} 20 \log_{10}(r), & r < 1000 \\ 60 + 10 \log_{10}(r/1000) + 0.005\, r, & r \geq 1000 \end{cases},$$

and $\beta(r)$ is the spread in transmission loss

$$\beta(r) = 10 \log_{10}\left(\frac{r}{1000}\,\frac{\pi^2}{6}\right),$$

also measured in dB units. A plot of the probability density function of the transmission loss at ranges of 1000, 2000 and 5000 yd is shown in figure 7.14. The spread in the probability density function rapidly increases with range.

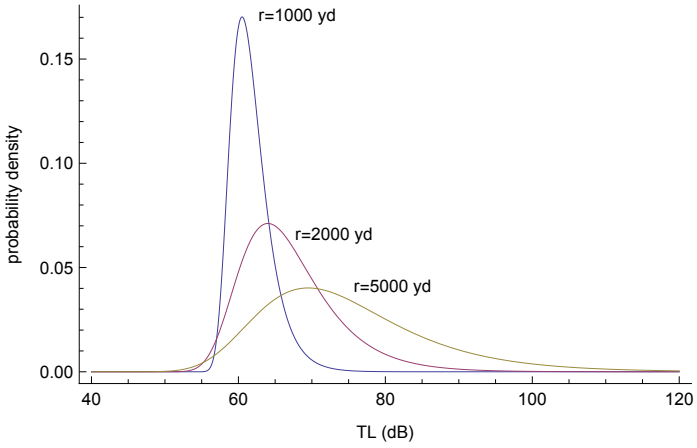

Figure 7.14. Probability density of transmission loss at 1000 yd, 2000 yd and 5000 yd.

The expected probability of detection at range r can be found by marginalizing over the probability

density in transmission loss. The result is

$$\overline{p}_d(r) = \int_0^\infty (p_{\text{fa}})^{\frac{1}{1+10^{\frac{SL-TL-AN}{10}}}} f_{TL}[TL, \alpha, (r), \beta)\,(r)]\, d TL$$

If there were uncertainty in the prediction of the ambient noise level AN, then $\overline{p}_d(r)$ would be defined by

$$\overline{p}_d(r) = \int_0^\infty \int_0^\infty (p_{\text{fa}})^{\frac{1}{1+10^{\frac{SL-TL-AN}{10}}}} f_{TL}[TL, \alpha, (r), \beta)\,(r)]\, f_{AN}(AN)\, d TL\, d AN$$

where $f_{AN}(AN)$ is the probability density function of the ambient noise level AN.

The variance of the probability of detection at range r assuming only uncertainty in the transmission loss is defined by

$$\sigma^2_{p_d}(r) = \int_0^\infty \left((p_{\text{fa}})^{\frac{1}{1+10^{\frac{SL-TL-AN}{10}}}} \right)^2 f_{TL}[TL, \alpha, (r), \beta)\,(r)]\, d TL - [\overline{p}_d(r)]^2.$$

Figure 7.15 shows a plot of the expected probability of detection $\overline{p}_d(r)$ and bounds that are one standard deviation $\sigma_{p_d}(r)$ wide. There is so much spread in the transmission loss probability density function that it is not worthwhile to compute probability of detection intervals that are two standard deviations wide. Thus in this particular case Chebyshev's theorem is not useful to us because of the large size of $\sigma_{p_d}(r)$, but in many circumstances it will be.

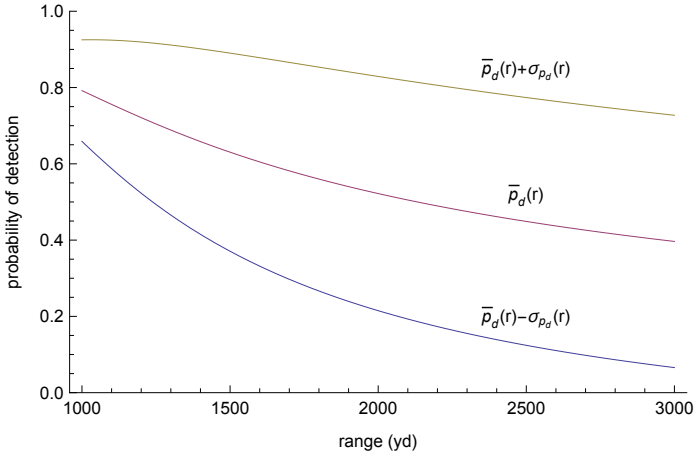

Figure 7.15. Effect of uncertainty in transmission loss on estimation of probability of detection.

References

Blake, Lamont V. (1991), *Radar Range-Performance Analysis*, Munro Publishing Co.

Brekhovskikh, L. and Lysanov, Yu. (1982), *Fundamentals of Ocean Acoustics*, Springer Verlag.

Burdic, William S. (1984), *Underwater Acoustic System Analysis*, Prentice-Hall.

Elmore, W.C. and Heald, A.H. (1969), *Physics of Waves*, Dover Publications.

Gregory, Phil (2005), *Bayesian Logical Data Analysis for the Physical Sciences,* Cam ridge University Press.

Hammersley, J.M. and Handscomb, D.C. (1964), *Monte Carlo Methods*, Chapman and Hall.

Hogg, R.V. and Tanis, E.A. (2006), *Probability and Statistical Inference*, Pearson Prentice Hall, 7th edition.

Hudson, J.A. (1980), *The Excitation and Propagation of Elastic Waves*, Cambridge University Press.

Jaynes, E.T. (2003), *Probability Theory: The Logic of Science*, edited by G. Larry Bretthorst, Cambridge University Press, reprinted 2009.

Jeffreys, Harold, (1973), *Scientific Inference*, Cambridge University Press, 3rd edition.

Jeffreys, Harold, (1976), *The Earth: Its Origin, History and Physical Constitution*, Cambridge University Press, 6th edition.

Jensen, F.B., Kuperman, W.A., Porter, M.B. and Schmidt, H. (1994), *Computational Ocean Acoustics*, American Institute of Physics.

Kimall, G.E. and Morse, P. M. (1970), *Methods of Operations Research*, Peninsula Publishing.

Koopman, Bernard O. (1980), *Search and Screening*, Pergamon Press, republished by The Military Operations Research Society 1999.

Officer, C.B. (1958), *Introduction to the Theory of Sound Transmission*, McGraw-Hill Book Company.

Ol'shevskii, V.V. (1978), *Statistical Methods in Sonar*, technical editor David Middleton, Studies in Soviet Science, Consultants Bureau.

Rees, W.G. (2001), *Physical Principles of Remote Sensing*, Cambridge University Press, 2nd edition.

Ross, Sheldon M. (1972), *Introduction to Probability Models*, Academic Press.

Selin, Ivan. (1965), *Detection Theory*, Princeton University Press.

Skudrzyk, E. (1971), *The Foundations of Acoustics*, Springer-Verlag.

Tucker, D.G. and Gazey, B.K. (1977), *Applied Underwater Acoustics*, Pergamon Press.

Urick, Robert J. (1983), *Principles of Underwater Sound*, McGraw-Hill Book Company.

Whalen, Anthony D. (1971), *Detection of Signals in Noise*, Academic Press.